

Chapter 27

Scrotal Imaging



Michal Yaela Schechter, Erik Van Laecke, and Anne-Françoise Spinoit

Abbreviations

CT	Computed tomography
CEUS	Abdominal contrast-enhanced ultrasound
GCNIS	Germ cell neoplasia in situ
GCT	Germ cell tumor
MRI	Magnetic resonance imaging
NSGCT	Non-seminomatous germ cell tumor
SCST	Sex cord-stromal tumor
US	Ultrasound

27.1 Introduction to Scrotal Imaging

The scrota contain complex anatomical, vascular, lymphatic, and innervation systems which aid its multiple functionalities including reproduction, thermoregulation, and endocrine hormone production. Clinical examination is critical for proper evaluation of the scrotum and may be aided by imaging, particularly when physical exam findings are equivocal.

Basic scrotal imaging involves the following modalities: Ultrasound (US), Doppler, Magnetic Resonance Imaging (MRI), and Computed Tomography (CT). Each technique is different in terms of the images it gathers, equipment required, and the conditions it may be used in.

US imaging, also called a sonogram, is one of the safest forms of medical imaging, and is quite cost-effective as well. It uses high-frequency sound waves

Michal Y. Schechter is fully funded by the Gianni Eggermont fund for advancement of research in Pediatric Urology.

M. Y. Schechter · E. Van Laecke · A.-F. Spinoit (✉)
Department of Urology, Ghent University Hospital, ERN eUROGEN Accredited Centre,
Ghent, Belgium

which reflect off soft tissue to generate images of organs and other bodily structures. A subset of ultrasound imaging is known as doppler imaging, which uses sound waves to allow visualization of blood flow in arterial and venous vasculature.

CT imaging uses serial X-rays to produce 3D images of bones, organs, blood vessels, and other soft tissues within the body. While these scans were created to provide more detailed images than conventional X-rays, they also produce more radiation and are therefore limited in their use in children. However, the ongoing evolution of CT imaging has since created better imaging with limited radiation doses, and these improvements are expected to further develop in the future.

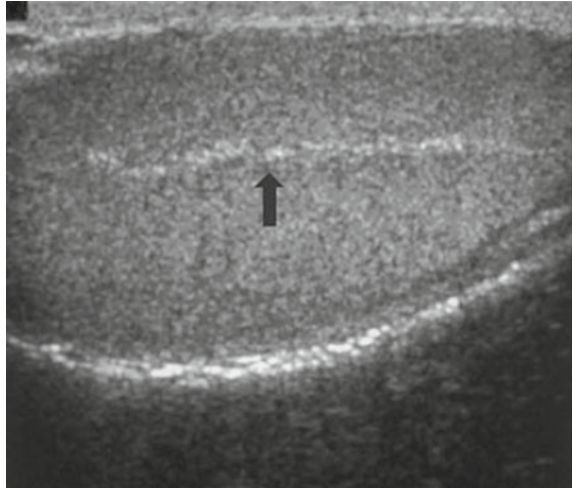
MRI scans are one of the highest quality imaging modalities available. These scans use a strong magnetic field along with radio waves to create 3D images of the body and realize differences in tissue that would not otherwise be seen with a CT scan. MRI is similar to CT in that they can both create cross-sectional imaging of the body but is different in that MRI does not use harmful radiation. MR imaging can also create higher quality images than CT, enabling it to better highlight differences in tissues. However, an MRI takes a considerably longer amount of time to scan than does a CT and is more expensive.¹

Indications for imaging include scrotal abnormalities, pain, trauma, masses, infertility, and follow-up. As the scrota and its contents are relatively superficial, an ultrasound scan can produce quite detailed and accurate information and is therefore the primary imaging technique used for scrotal evaluation after initial clinical examination. Typical adults have a scrotal thickness of about 2–8 mm, with each testis measuring 3–5 cm in diameter and about 20 mL in volume.² Testicular volume evolves with pediatric growth curves, with a linear increase in volume related to pubertal physical growth and usually considered to be the first sign of the puberty.

Normal ultrasound findings show the testis as a structure with homogenous echogenicity containing a mildly coarse echotexture. The tunica vaginalis and albuginea appear as an echogenic outline of the testis, and the mediastinum testis is visualized as a linear echogenic invagination of the tunica albuginea. A minority of patients have an identifiable rete testis which can form a hypoechoic region near the mediastinum. The epididymis appears isoechoic or mildly hyperechoic relative to the testis. On doppler imaging, the testis and epididymis demonstrate a low-resistance arterial velocity. The appendix testis and appendix epididymis are not usually noticeable unless paratesticular fluid is present.

MRI is the imaging method of choice when US characterization of the lesion is insufficient. CT scans are performed less frequently than MRI and are mainly used for testicular neoplasm staging and treatment follow-up. MR Imaging of normal scrota demonstrates intermediate testicular signal intensity on T1-weighted images, with a low signal intensity of the tunica albuginea and a heterogenous and isointense epididymis relative to the testis. On T2-weighted images, normal testes have high signal intensity with low signal intensity of the tunica albuginea, as well as a hypointense epididymis, making this the best MRI format for epididymal visualization and differentiation from the adjacent testis. Contrast-enhanced scrotal MRI

Fig. 27.1 Normal scrotal US with mediastinum testis (arrow) visualized as a linear echogenic band³



demonstrates homogenous testicular enhancement and can best show the rete testis radiating from the mediastinum testis to the tunical surface.

When imaging a scrotum it is critical to also assess the contralateral scrotum, both for ensuring that it is not pathologic and because the comparison between the scrotum may aid in evaluation of the scrotum in question (Figs. 27.1 and 27.2).

27.2 Acute Scrotum

Cases of acute scrotum include acute epididymitis/epididymo-orchitis, testicular torsion, appendiceal torsion, and trauma. The first step in evaluation of acute scrotum is performance of an US. Acute scrotum may also include Fournier gangrene.

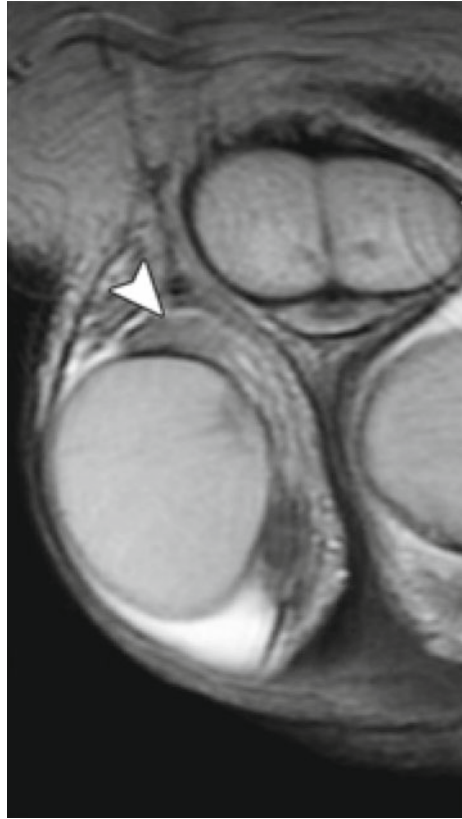
Infection

Infection is the most common cause of an acute scrotum, and can include the epididymis (epididymitis), testis (orchitis), or if the infection spreads it can include both the epididymis and the testis (epididymo-orchitis).

Acute epididymitis typically appears on US as an enlarged hypo/hyperechoic epididymis along with heterogenous echogenicity secondary to diffuse testicular spread of the infection. While these findings are nonspecific, epididymo-orchitis is the most common disease with these combined findings on US. Cases may also exhibit indirect signs of inflammation such as scrotal wall thickening and reactive hydrocele.

The discerning urologist should keep in mind that a heterogenous testicular echotexture is not pathognomonic to epididymo-orchitis. Although neoplastic

Fig. 27.2 Normal scrotal T2-weighted MRI, with hypointense epididymis (arrowhead)⁴



lesions are usually found in one testis while infection may be unilateral or bilateral, cases of testicular leukemia and lymphoma may have a similar appearance on US to epididymo-orchitis. As heterogeneous echogenicity does not always indicate scrotal infection, suspected cases should be monitored with a follow up US after their resolution to rule out neoplasms or infarctions.

The hallmark of doppler in epididymo-orchitis is increased blood flow, consistent with hyperemia of the epididymis, testis, or both. As grey-scale US findings can be within normal limits in cases of testicular infection and doppler has a nearly 100% sensitivity for scrotal inflammation detection, hyperemia in Doppler US can be used as a diagnostic tool in epididymo-orchitis cases.⁵ Careful comparison with the contralateral asymptomatic testis is important to ensure that the doppler imaging is properly working to detect blood flow (Fig. 27.3).

Testicular Torsion

Testicular torsion is considered a medical emergency of testicular ischemia, attributable to venous obstruction followed by arterial obstruction. The terminal nature

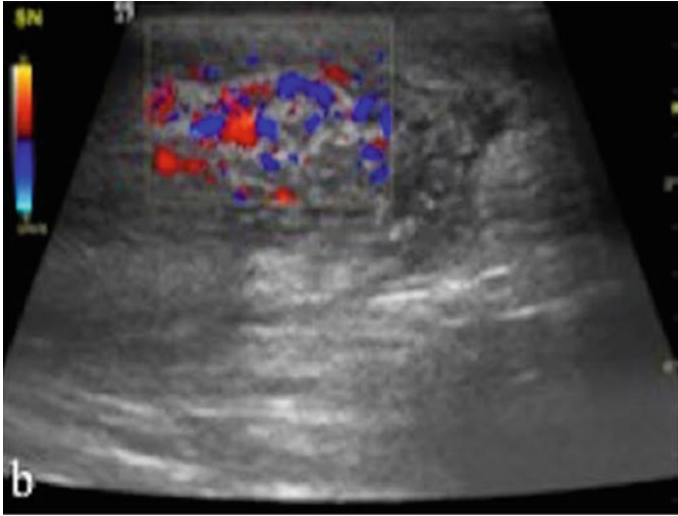


Fig. 27.3 Acute epididymitis on doppler US, showing a heterogeneous echotexture with increased blood flow⁶

of testicular vascularization as outlined in the anatomy of scrotum chapter is critical for the development of torsion of the testis.

Two incidence peaks have been described, correlating with two different types of torsion: Extravaginal testicular torsion in neonates and intravaginal testicular torsion typically occurring in adolescents. Extravaginal torsion is caused when the tunica vaginalis is not affixed to the gubernaculum, increasing torsion risk of both the tunica vaginalis and the spermatic cord. Neonates with this condition typically present at birth with an already infarcted and necrotic testis. Intravaginal torsion occurs within the tunica vaginalis and often affects adolescents with bell-clapper deformity, a condition in which the tunica vaginalis attaches at a point higher than the posterolateral testis, allowing the spermatic cord to twist inside.

The diagnosis of testicular torsion is mostly clinical. If additional investigation is needed, an US should be performed urgently as the testicular salvage rate is dependent not only on the degree of torsion, but also on the duration of vascular congestion and ischemia. A 90–100% salvage rate with performance of detorsion exists within the first 6 hours after onset of symptoms, a 20–50% rate within 12–24 hours, and a 0–10% rate after 24 hours.⁷

Cases of suspected testicular torsion should be evaluated with a doppler study, the hallmark of which is an absence of intratesticular blood flow. This single criterion is 86% sensitive and 100% specific for a torsion diagnosis.⁸ In some cases, paratesticular flow in epididymal collaterals also appears within hours of the onset of torsion. As with cases of testicular infection, careful comparison with the contralateral asymptomatic testis is important to ensure that the doppler imaging is properly working to detect blood flow.

The doppler component of the ultrasound is especially critical as grey-scale US findings are nonspecific for torsion and are often normal in the early phases of torsion. At 4–6 hours post onset of torsion, a common grey-scale US finding is testicular swelling and decreased echogenicity. Infarction can alter testicular echogenicity and is therefore used to help predict testicular viability. A case of late or missed torsion (24 hours post onset) is typically visible as an increasingly heterogenous testicular echotexture. Other US findings in torsion cases may include an enlarged hypoechoic epididymal head (secondary to torsion of the deferential artery which feeds the epididymis), an abnormally round or oval homogenous spermatic cord caudal to the point of torsion (secondary to twisting of the spermatic cord at the level of the superficial inguinal ring), and indirect signs of inflammation similarly found in testicular infection.⁹

Recently, near infrared spectroscopy has shown promising results in experimentation for testicular torsion diagnosis. It can provide a quicker diagnosis than a doppler and it measures the testicular O₂ saturation which can be more useful than the blood flow as measured by a doppler.¹⁰ It remains to be seen whether this imaging modality will be widely implemented (Fig. 27.4).

Trauma

Scrotal trauma can include testicular rupture, fracture, or hematomas. US is used in these cases to help inform which scrotal injuries warrant surgical intervention. Abdominal contrast-enhanced ultrasound (CEUS) is a form of US imaging that uses gas-filled microbubbles to better visualize abdominal and pelvic organs and blood vessels and can provide superior results to both grey-scale US and CT. It may be used as a rapid imaging modality in emergency cases that require more accurate identification of viable tissue to determine if surgical intervention is warranted.

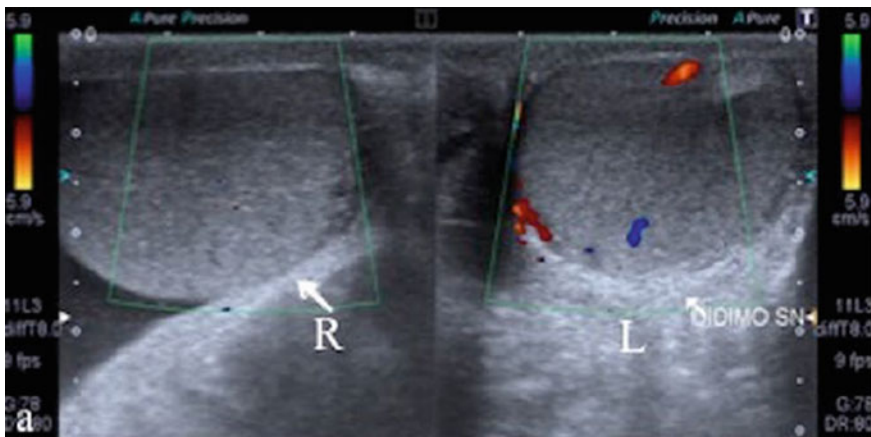


Fig. 27.4 Testicular torsion on doppler US, showing absence of flow in the R testis as opposed to the L testis¹¹

A testicular rupture is a surgical emergency that occurs when a tear in the tunica albuginea allows for extrusion of testicular contents. Exploratory surgery performed within 72 hours after the trauma can save up to 90% of ruptured testes. It should be noted that the tunica albuginea and the tunica vasculosa are situated right next to each other, so rupture of the tunica albuginea often also causes vascular loss to the testis due to the concurrent rupture of the tunica vasculosa. The main US findings include a heterogeneous testicular echotexture with irregular poorly defined borders due to hemorrhage and necrosis, contour abnormality due to testicular parenchyma extrusion, disruption of the tunica albuginea, and a large hematocele. The first two US findings of testicular heterogeneity with contour abnormality have a sensitivity of 100% and a specificity of 93.5%. Doppler US can demonstrate disruption of the normal blood flow of the tunica vasculosa (Fig. 27.5).¹²

Another scrotal surgical emergency is testicular fracture, which refers to a break in the normal testicular parenchyma that appears on US as a linear hypoechoic and vascular area within the testicular parenchyma. While it may be associated with a ruptured tunica albuginea and therefore become a case of testicular rupture, a fracture without rupture is contained within the testicular parenchyma. US doppler is critical in delineating the extent of viable tissue to determine salvageability and management. However, direct visualization of a fracture line is uncommon. When conventional ultrasound findings are equivocal, CEUS can both better define



Fig. 27.5 Testicular rupture on US, with heterogenous echotexture and contour abnormality (arrows)¹³

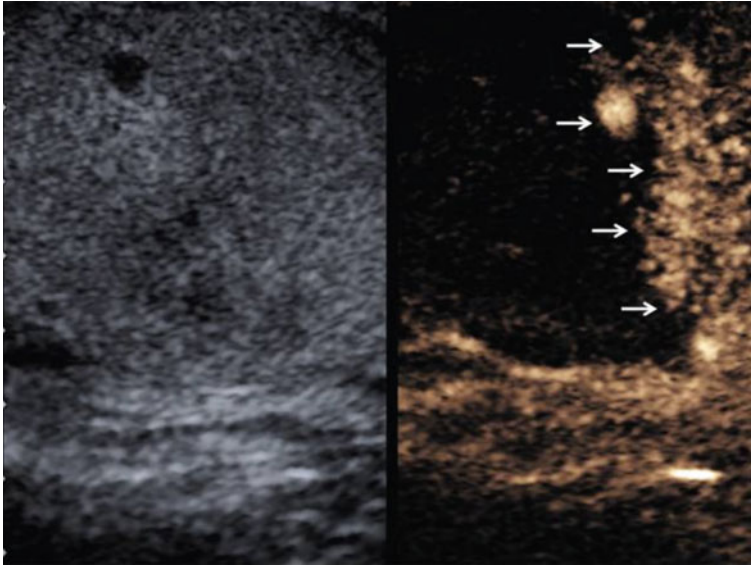


Fig. 27.6 Testicular fracture on US (left) and CEUS (right), with a clear demarcation between vascularized and non-vascularized tissue (arrows)¹⁵

fracture lines and differentiate between enhancing viable vascularized tissue and nonenhancing nonvascularized tissue (Fig. 27.6).¹⁴

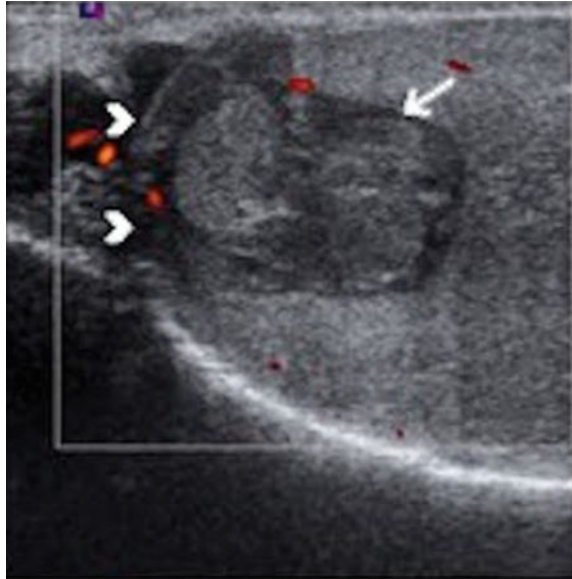
Post-traumatic testicular hematomas may present as intratesticular hematomas, extratesticular hematomas in the epididymis and scrotal wall, or as hematoceles (hematomas between the visceral and parietal layers of the tunica vaginalis). US appearance of hematomas varies with time. Acute hematomas on US appear more hyperechoic and may have a diffusely heterogenous mixture, but as these hematomas become chronic and resolve, they decrease in their echogenicity and size and become more complex with cystic components. On doppler, intratesticular hematomas appear as focal areas of avascularity (Fig. 27.7).¹⁶

There are a few caveats in the management of a suspected acute hematoma. If an acute hematoma is suspected but imaging is negative, repeat imaging should be performed within 12–24 hours after the initial US evaluation, as the initial echotexture of a hematoma may be indistinguishable from the surrounding parenchyma.

As mentioned earlier, the testicular parenchyma underlies the tunica albuginea and an injury to one structure very often means an injury to the other as well. However, a heterogeneous intratesticular lesion may appear in cases of intratesticular hematomas without testicular rupture. These cases require imaging, in particular a CEUS, to better assess if surgical exploration for testicular rupture is warranted.

Finally, about 10–15% of testicular tumors first manifest and are incidentally discovered after scrotal trauma.¹⁸ This is likely because testicular tumors are the

Fig. 27.7 Intratesticular hematoma on doppler US, with an avascularized, hypoechoic, and heterogenous echotexture (arrows) with an intact tunica vaginalis (arrowheads)¹⁷



most common solid malignancy in 15–35-year-old males, and the highest incidence of traumatic injury is in that age group. Testicular tumors often appear similarly to hematomas, and in cases of trauma it can be difficult to differentiate between lesions. Therefore, cases with abnormal intratesticular US readings without immediate surgical intervention should be followed up with a repeat US to rule out malignancy, as over time scrotal hematomas are expected to shrink and scrotal masses are expected to grow. If US findings are equivocal, MRI may be used for a more conclusive diagnosis.

Appendiceal Torsion

US evaluation of torsion of the appendix testis or appendix epididymis is useful in terms of excluding testicular torsion and acute epididymo-orchitis. A classic physical examination finding in cases of appendiceal torsion is the “blue dot sign”, referring to a small firm nodule palpable on the upper pole of the testis presenting as a bluish discoloration through the overlying skin. US typically shows a hypo or hyperechoic mass in comparison to the echotexture of the adjacent testis or epididymis, and these findings are often associated with a reactive hydrocele and scrotal skin thickening. Color doppler with no internal blood flow and increased peri-appendiceal peripheral flow is highly suggestive of appendiceal torsion (Fig. 27.8).¹⁹

Fournier Gangrene

Fournier gangrene is a fulminant necrotizing fasciitis caused by mixed aerobic and anaerobic bacteria that frequently extends to the perineal, perianal, and lower abdominal wall regions. This condition typically presents in adults with high

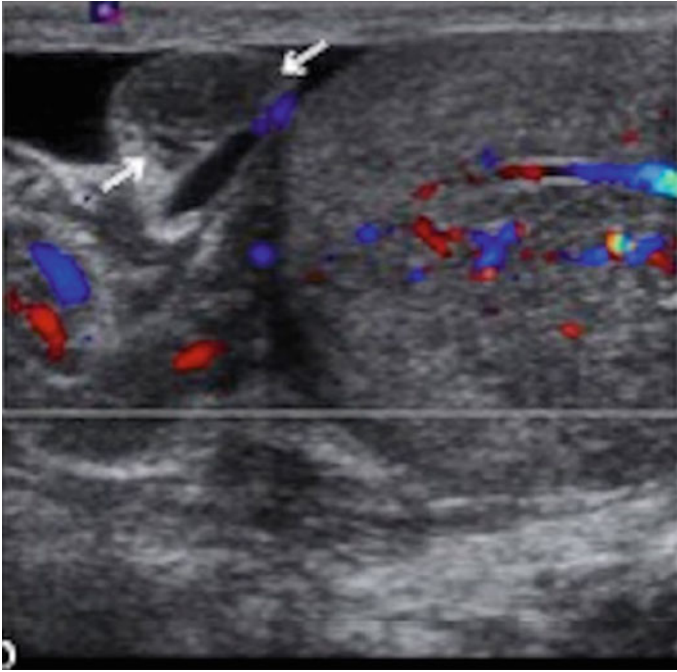


Fig. 27.8 Appendiceal torsion on doppler US, with an enlarged and avascularized mass (arrows)²⁰

comorbidities such as diabetes, obesity, and alcoholism. As rapid progression of tissue necrosis can lead to multiorgan failure and a mortality rate of up to 75%,²¹ this condition constitutes a urologic emergency necessitating prompt diagnosis and initiation of surgical debridement and antibiotics. Fournier gangrene is a clinical diagnosis and treatment should not be delayed for imaging confirmation unless exam findings are ambiguous. Characteristic crepitus can present at physical exam in 19–64% of patients.²²

Imaging techniques include US and CT in determining the location and cause of scrotal gas when clinical signs cannot produce a definitive diagnosis. CT is the preferred modality of imaging and demonstrates soft tissue thickening, fat stranding, and subcutaneous emphysema dissecting the fascial layers. Although US is not considered first-line imaging in suspected cases, it can still help with early disease recognition in emergency department settings. The hallmark of Fournier gangrene on US is multiple hyperechoic and hyperreflective foci with posterior acoustic dirty shadowing relating to the underlying subcutaneous gases within the scrotal wall. Other US findings include scrotal wall swelling and thickening, with doppler showing increased blood flow in the affected area (Fig. 27.9).

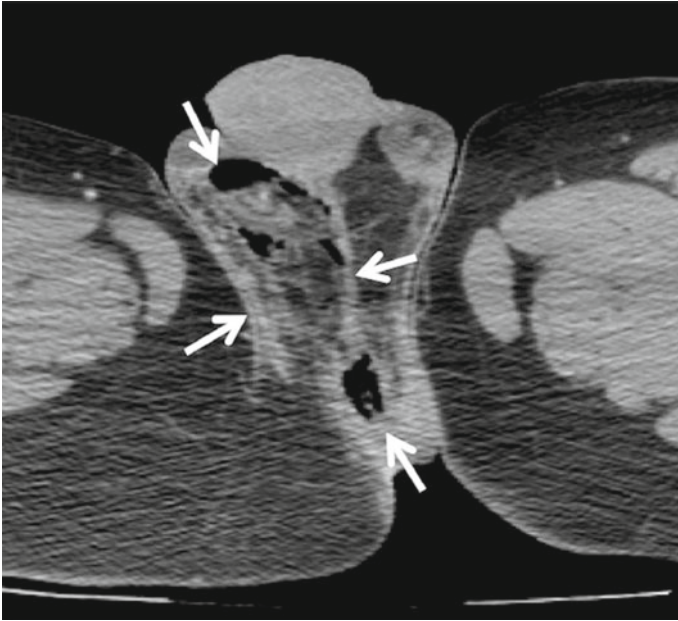


Fig. 27.9 Fournier gangrene on CT, with inflammation and gaseous changes in the scrotal wall (arrows)²³

27.3 Scrotal Masses

The initial classification of a scrotal mass as intratesticular or extratesticular is important because intratesticular masses are considered cancerous until proven otherwise, while extratesticular masses are rarely malignant (3%).²⁴ US is the primary imaging modality used to assess the location of scrotal masses, with the possibility of vascularity assessment through use of doppler. When US findings are indeterminate, MR imaging can act as an adjunctive diagnostic tool and help localize the lesion as well as evaluate for local tumor extension and regional spread. CT imaging is used to assess the presence of metastases and determine tumor resectability. CT also plays a pivotal role in tumor surveillance and evaluation of response to treatment.

Extratesticular cysts appear similarly to intratesticular cysts on US and doppler. The differentiation of intra and extratesticular cysts does not have clinical significance, and purely cystic cancers are extremely rare.

27.3.1 Extratesticular Masses

The variety of scrotal structures surrounding the testicle can give rise to several types of extratesticular masses. Malignant neoplasms are rare and can include rhabdomyosarcomas, leiomyosarcomas, and liposarcomas. The more commonly found benign neoplasms are lipomas, adenomatoid tumors, and leiomyomas. Extratesticular cysts include epididymal cystic masses and hydroceles. Another form of an extratesticular benign mass is an inguinal hernia.

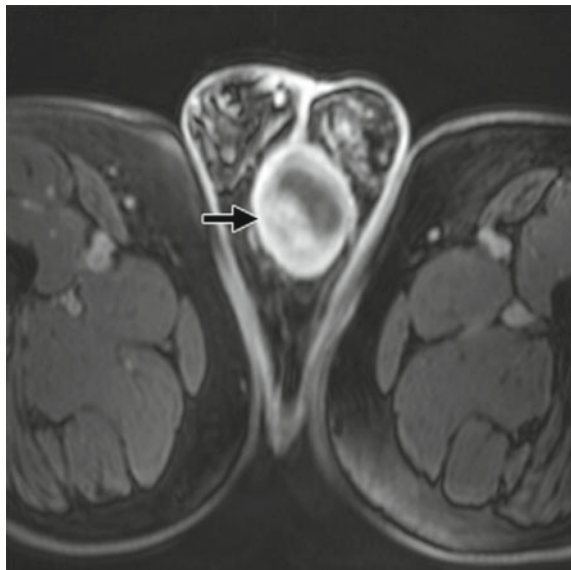
Rhabdomyosarcoma, Leiomyosarcoma, and Liposarcoma

Rhabdomyosarcoma is a pediatric malignancy which has nonspecific findings on MRI. It typically presents as an encapsulated gray-white mass with focal areas of hemorrhage and cystic degeneration and cannot be well-differentiated from other malignant or benign extratesticular neoplasms. Leiomyosarcoma appears on US and CT as a heterogenous enhancing mass and can be evaluated for tumor spread with MRI. Due to its fat content, liposarcoma has nonspecific hyperechoic findings on US but CT and MRI can be used to better determine its presence and show well-defined macroscopic fat masses (Fig. 27.10).

Lipoma, Adenomatoid Tumor, and Leiomyoma

Lipomas are the most common extratesticular non-malignant neoplasm. They appear on US as well-defined homogenous hyperechoic masses and are absent of blood flow on doppler. Adenomatoid tumors are visualized on US as well-defined hypoechoic masses with variable doppler flow. Leiomyomas are rare and present on US as solid isoechoic lesions with shadowing at transition zones.²⁶

Fig. 27.10 Liposarcoma of the spermatic cord on T1-weighted MRI, showing as an enhanced scrotal mass (arrow)²⁵



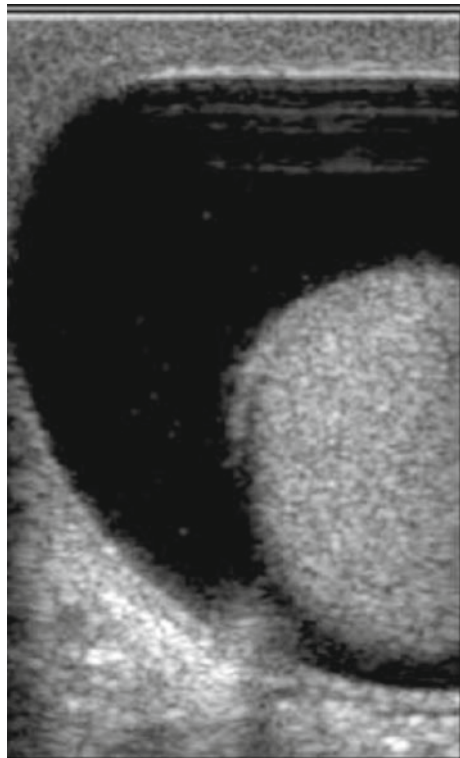
Epididymal Cystic Masses

Epididymal masses can be further categorized into a single epididymal cyst or a spermatocele, which is a cystic dilation of the tubular efferent ductules in the head of the epididymis. Single epididymal cysts are made up of clear serous fluid, while spermatoceles can be multilocular and contain proteinaceous fluid and spermatozoa. It should be noted that all cysts lack internal vascularity on doppler. These two subtypes appear as well-defined, homogeneous, hypoechoic lesions with posterior acoustic enhancement on US. Although imaging cannot be used to accurately distinguish one from another, this does not present a challenge as these conditions usually do not have clinical relevance.

Hydrocele

Hydroceles are the most common cause of painless scrotal swelling and can present either as congenital lesions due to a patent processus vaginalis or in their adult form which may be associated with underlying scrotal pathology. This diagnosis is confirmed by an US exam where they are visualized as anechoic fluid collections around the anterolateral testis (Fig. 27.11).

Fig. 27.11 Hydrocele on US, showing as a peritesticular fluid collection²⁷



Inguinal Hernia

Inguinal hernias typically consist of bowel or omentum. Bowel hernia appearance is dependent on bowel content. US imaging showing specular reflection within fluid indicates bowel containing fluid, while bowels containing air or solid stool appear with a bright echotexture. US also allows for visualization of peristalsis within the bowel hernia, thus establishing the diagnosis. Omental hernias can be visualized on US as paratesticular masses with diffuse echotextures due to their fat content.²⁸

27.3.2 Intratesticular Masses

Intratesticular scrotal masses include testicular neoplasms and cysts. Testicular cancer is the most common neoplasm found in men aged 15–40 years old. It accounts for 1–2% of all neoplasms in males. Testicular cancer can also present in the pediatric population, in particular during the neonatal period and puberty, accounting for 2–4% of childhood cancers.³⁰

Testicular tumors may arise from germ cells, sex cord-stroma, or lymph, and are classified based on their origins. 90–95% of testicular tumors are germ cell tumors (GCTs), which are further categorized based on the most recent 2016 WHO classification system regarding their derivation status from germ cell neoplasia in situ (GCNIS). The classification system of testicular tumors is critical as it guides their treatment and determines the prognosis. It includes testicular GCTs derived from GCNIS, testicular GCTs not derived from GCNIS, non-germ cell testicular tumors: sex cord-stromal tumors, and hemato-lymphoid tumors. It should be noted that GCNIS tumors have a tendency for invasion and have been found in the contralateral testis in up to 8% of patients with GCNIS.³² Overall, GCNIS tumors are more typically found in the adult population as opposed to the pediatric population, and vice-versa for non-GCNIS tumors which are more common in children. There is growing evidence that testicular prepubertal tumors and postpubertal tumors differ both in terms of clinical features and prognosis.

Intratesticular cysts include cysts of the tunica albuginea, tubular ectasia of the rete testis, and testicular cysts. Another type of testicular mass includes testicular microlithiasis.

When combined with a clinical examination, US has been shown to have a nearly 100% sensitivity in diagnosis of testicular cancer.³³ Doppler can show hypervascularity in the majority of cases involving malignant tumors, but an absence of blood flow cannot be used for exclusion of malignancy as it is more difficult to demonstrate increased vascularity in small tumors. Although MRI does not have a clear diagnostic benefit in testicular cancer as compared to US, it is helpful in cases where US findings are equivocal. MRI can help differentiate seminomatous GCTs from their nonseminomatous counterparts by demonstrating seminomatous GCTs as homogeneously T2 hypo- and T1 isointense masses along with internal T2 hypointense bands which enhance more than the tumor.

Non-seminomatous GCTs present with T1 and T2 heterogeneous appearance on MRI and may be associated with a T2 hypointense fibrous pseudocapsule.

Testicular GCTs Derived from GCNIS

This classification includes pure seminoma along with non-seminomatous (NSGCT) tumors such as embryonal carcinoma, choriocarcinoma, postpubertal type teratoma, and regressed GCTs. While NSGCTs are typically found in pure form in the pediatric population, adult NSGCTs often present as mixed GCTs and contain two or more different histological GCT components. Mixed GCTs appear on US as ill-defined masses with a heterogenous echotexture and possible echogenic foci.

Seminoma

Pure seminomas make up about 50% of all testicular GCTs. Sonographically, seminomas appear as homogenous hypoechoic solid lesions and rarely invade paratesticular tissues. If multilobulated, they show increased blood flow on doppler along their echogenic fibrinous septae (Fig. 27.12).

Embryonal Carcinoma

Embryonal carcinoma is an aggressive tumor which extends into the extratesticular space and distorts the contour of the testis in about 25% of cases.³⁵ US imaging typically shows ill-defined predominantly hypoechoic lesions with widespread necrosis, hemorrhage, and fibrosis (Fig. 27.13).

Choriocarcinoma

Choriocarcinoma is a highly malignant tumor composed of both cytotrophoblasts and syncytiotrophoblasts and represents the form of testicular cancer with the highest mortality. It has a propensity for early vascular invasion leading to hematogenous dissemination, particularly to the lungs. On US, choriocarcinoma appears as a solitary mass or multifocal ill-defined heterogenous masses with mixed

Fig. 27.12 Pure seminoma on US, with multilobulated hypoechoic masses separated by fibrinous septae (dotted arrow)³⁴

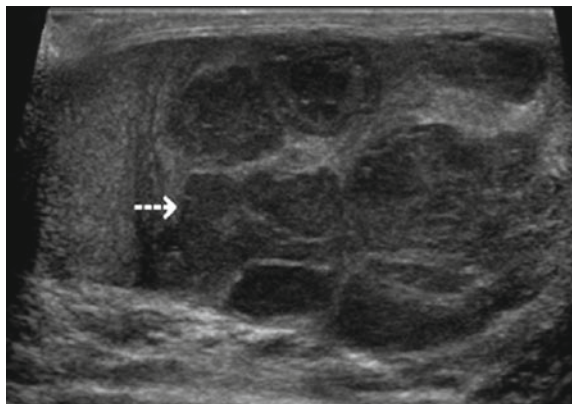


Fig. 27.13 Embryonal carcinoma on US, showing extension into the extratesticular space (dotted arrow)³⁶

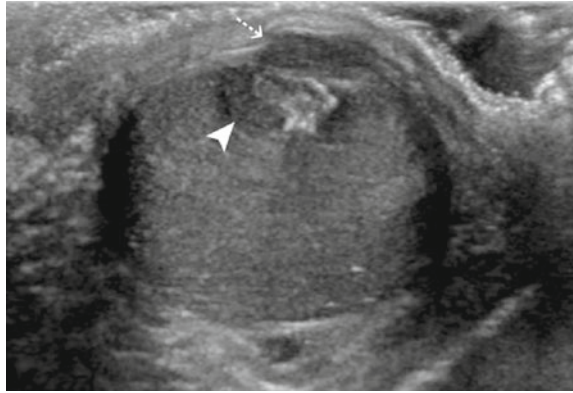
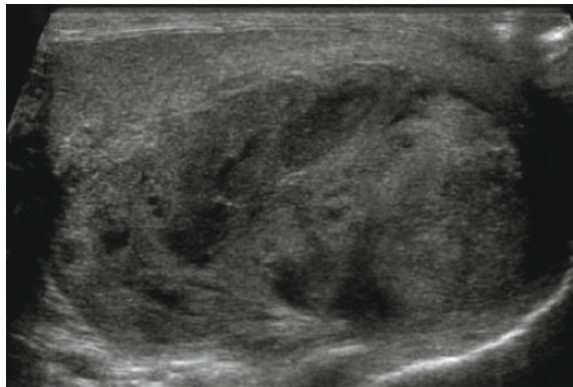


Fig. 27.14 Choriocarcinoma on US, showing an ill-defined heterogenous solid mass with necrosis³⁷



cystic and solid components due to hemorrhagic necrosis in the center of the tumor (Fig. 27.14).

Postpubertal-Type Teratoma

Postpubertal type teratoma is more common than the prepubertal type, and unlike the prepubertal type it is often malignant. Teratomas are composed of fetal tissue derived from all three germ cell layers (ectoderm, mesoderm, and endoderm) and present sonographically as large complex heterogenous masses with focal echogenic lesions. These lesions can represent cysts, fibrosis, calcifications, immature bone, and cartilage (Fig. 27.15).

Burned-Out GCTs

Burned-out GCTs represent tumors with a high metabolism, resulting in outgrowth of their blood supply and tumor regression. Appearance on US varies from a hypoechoic mass to small echogenic foci. These masses are typically discovered while searching for a primary source of retroperitoneal GCTs. The testicular

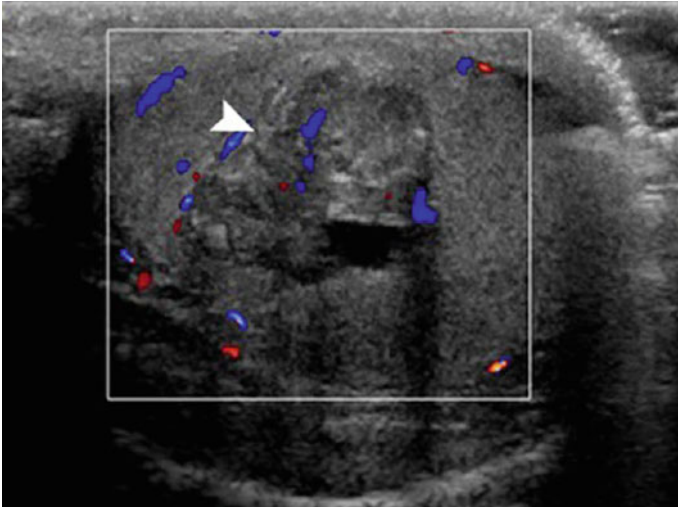
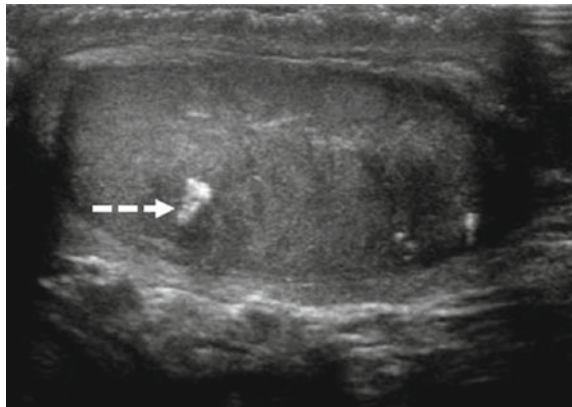


Fig. 27.15 Postpubertal teratoma on doppler US, as a complex heterogeneous mass with calcifications and cystic lesions (arrowhead)³⁸

Fig. 27.16 Burned out GCT on US, showing as a small focal intratesticular calcification (dotted arrow)³⁹



primary tumor is thought to metastasize and then “burn out”, leaving its retroperitoneal metastases behind with only a small testicular scar or calcification to mark its origination. Therefore, the discovery of an irregular scar should prompt consideration for GCT regression (Fig. 27.16).

Testicular GCTs Not Derived from GCNIS

This category includes spermatocytic tumors, prepubertal-type teratomas (epidermoid cyst and dermoid), and prepubertal-type yolk sac tumors. Non-GCNIS GCT’s are more inert and less likely to metastasize than their GCNIS counterparts and are more often found in the pediatric population.

Spermatocytic Tumor

Spermatocytic tumors represent a highly curable non-GCNIS subtype. They present on US as well-defined hypoechoic heterogeneous masses containing cystic spaces due to hemorrhagic changes with necrosis. Linear calcification may be visualized at the tumor periphery. Spermatocytic tumors, previously termed spermatocytic seminomas, are difficult to distinguish from seminomatous lesions based on imaging alone (Fig. 27.17).

Prepubertal-Type Teratoma

In contrast to the postpubertal-type teratoma, the prepubertal-type is typically benign and does not metastasize. Included in this category are the epidermoid cyst and dermoid subtypes. Epidermoid cysts contain lamellar keratin and are visualized as encapsulated round to oval lesions on imaging. Sonographically, they appear with a characteristic “onion skin” appearance of alternating concentric rings of hypo and hyperechogenicity. Epidermoid cysts may also present on MRI with alternating low and high signal intensity areas on T1- and T2-weighted images, in addition to a “target sign” pattern on T1-weighted images due to the hyperintense central area of the lesion (Fig. 27.18).

Dermoid testicular cysts are much less common than epidermoid cysts and do not have malignant potential. They are visualized on US as a hypoechoic mass,

Fig. 27.17 Spermatocytic tumor on US, demonstrating a well-defined hypoechoic heterogeneous lesion (arrow)⁴⁰

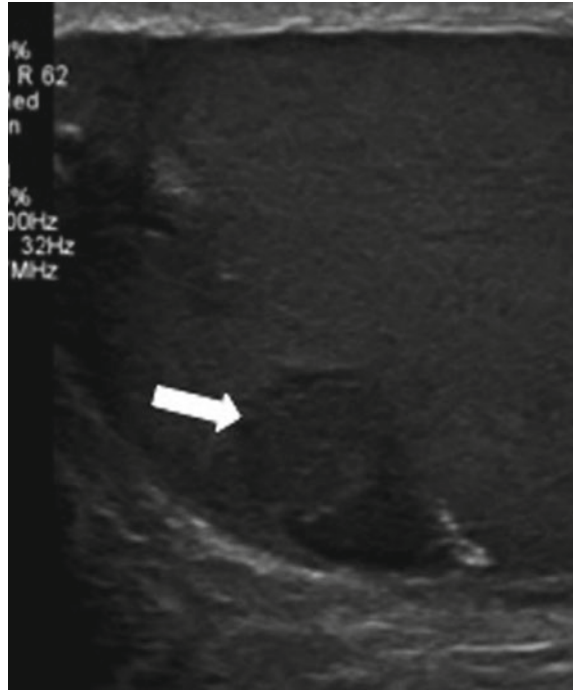


Fig. 27.18 Epidermoid cyst on US, showing an “onion skin” appearance. The author



possibly containing low-level echoes with tiny echogenic foci due to desquamated keratin crystals. Doppler imaging shows lack of internal vascularity.

Prepubertal-Type Yolk Sac Tumor

Prepubertal-type yolk sac tumors account for up to 80% of prepubertal malignant testicular tumors.⁴¹ US imaging shows a heterogenous appearance with varying proportions of cystic change and echogenic foci secondary to hemorrhage or necrosis. The prepubertal type is similar to the rarer postpubertal type, although the prepubertal type is a much more malignant subtype.

Non-Germ Cell Testicular Tumors: Sex Cord-Stromal Tumors

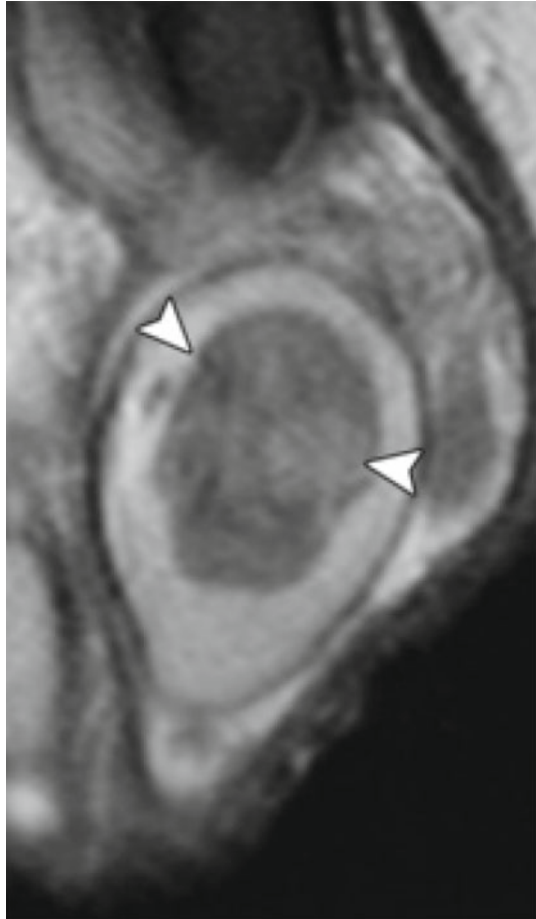
This testicular tumor classification includes sex cord-stromal tumors (SCSTs) including Leydig cell tumors and Sertoli cell tumors, and rarer subtypes such as granulosa cell tumors and other miscellaneous lesions.

Leydig and Sertoli Cell Tumor

As the most common type of SCST, Leydig cell tumors are commonly benign and can occur in any age group. As they appear on US as small hypoechoic masses and show increased blood flow on doppler, it is difficult to properly differentiate these tumors from seminomas based on US alone. Recently, MRI has been shown as superior to US in Leydig cell tumors diagnosis with a high sensitivity and specificity. Leydig cell tumor MRI demonstrates well-defined margins with a significant T2 hypointense signal and rapid and marked wash-in, which is then followed by a slow and late wash-out. Conversely, seminoma on MRI appears as a tumor with ill-defined margins and a mild T2 hypointensity, along with a weak, progressive wash-in without a wash-out. Additionally, Leydig cell tumor tumors may show a T2 hyperintense central scar on MR imaging with a capsular high T2 signal intensity (Fig. 27.19).

Sertoli cell tumors typically only present in patients less than 40 years old, with a minority of cases involving metastasis. US reveals increased echogenicity, with a dense collagenous matrix causing a multicystic “spoke wheel” pattern. MR imaging

Fig. 27.19 Leydig cell tumor on T2-weighted MRI, appearing as a hypointense intratesticular mass (arrowheads)⁴²

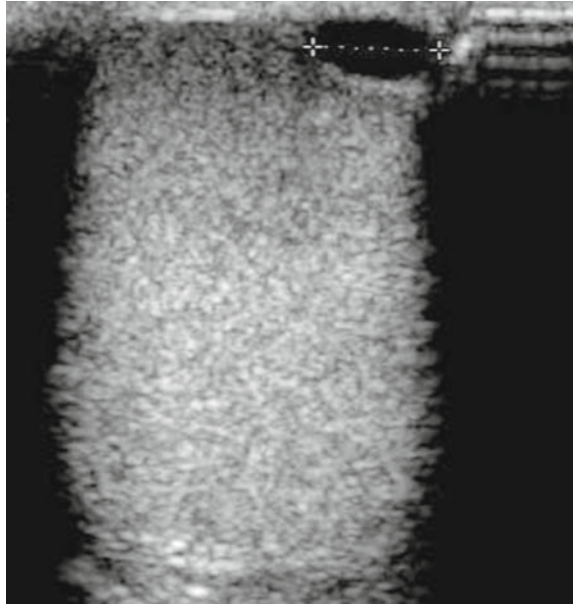


demonstrates a homogenous mass with intermediate T1 signal intensity lesions, hyperintense T2-weighted images, and rim enhancement.

Hemato-Lymphoid Tumor

Although lymphoma is a rare testicular tumor, it is the most common malignant testicular neoplasm in elderly men and is often secondary to non-Hodgkin lymphoma B-cell tumors. It is the most frequent bilateral testes neoplasm. Testicular lymphoma presents on grey-scale US as diffuse or focal hypoechoic lesions with increased vascularity on doppler. Some studies have described sonographic images of lymphoma as alternating hypo and hyperechoic striated bands radiating peripherally from the mediastinum testis.⁴³

Fig. 27.20 Cyst of the tunica albuginea on US, appearing as a well-defined anechoic space⁴⁴



Intratesticular Cysts

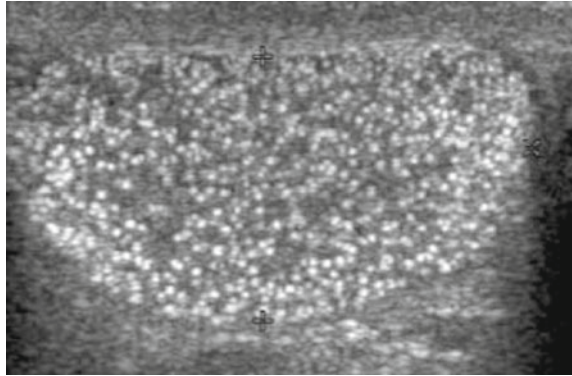
Intratesticular cysts include tubular ectasia of the rete testis and testicular cysts. These intratesticular cysts appear on US as typical cysts with well-defined anechoic structures. Tubular ectasia of the rete testes is a benign condition visualized on US as branching hypoechoic cystic figures in the mediastinum testis. It is important to accurately diagnose this condition on US as it can easily be confused with a hypoechoic mass and therefore cause an unnecessary biopsy (Fig. 27.20).

Testicular Microlithiasis

Testicular microlithiasis is an infrequently encountered condition involving intratubular calcifications. It is typically discovered incidentally on US and is visualized as echogenic foci 2–3 mm in size disseminated across the testicular parenchyma without acoustic shadowing. While some testicular microcalcification is considered normal, testicular microlithiasis is defined as the presence >5 foci per transducer field per testis. This condition has been associated with multiple urological conditions, most importantly testicular cancer which has been found in up to 44% of microlithiasis patients.⁴⁵ A cause-and-effect relationship between any of these associations has yet to be proven.

The association between microlithiasis and testicular neoplasms has produced much disagreement on how to best manage the uncertain status of microlithiasis as a precursor to carcinoma. Potential approaches including serial clinical examinations, US, tumor marker screenings, or immediate biopsy. The most recent recommendations are against follow up of isolated microlithiasis in the absence of a

Fig. 27.21 Testicular microlithiasis on US, visualized as multiple disseminated echogenic foci with no acoustic shadowing⁴⁷



solid mass or risk factors in the patient's history including maldescent, orchidopexy, testicular atrophy, or personal or family history of GCT. Some sanction annual serial US exams for microlithiasis patients up to age 55 years with risk factors and no solid mass (Fig. 27.21).⁴⁶

27.4 Infertility

Infertility is estimated to affect about 7% of the male population. The etiology of infertility can be challenging to identify, and half of all infertile men remain without a diagnosed etiology. Due to its ability to accurately present intrascrotal contents, ultrasonography is widely used as the primary imaging modality for assessment of male infertility and can assess for presence of varicocele, cryptorchidism, and testicular hypotrophy. US can also provide details on a number of conditions which are associated to varying degrees with male infertility, such as epididymitis, epididymal cysts, spermatoceles, testicular GCT's, and testicular microlithiasis. It should be noted that it is not uncommon for small testicular masses to incidentally be discovered during a workup of male infertility. These masses generally do not demonstrate substantial growth and may be safely observed with follow-up.⁴⁸

Varicocele

Varicoceles occur when the venous valves of the pampiniform plexus become ineffective. The resulting impairment in plexus drainage leads to its dilation and hyperthermia, causing a progressive decline in testicular function. As discussed in the anatomy of scrotum chapter, testicular venous drainage consists of a complex anastomotic and varying system which must be taken into consideration in cases of suspected varicocele. The variation in venous drainage on the left and right sides is clinically relevant for the pathogenesis of varicocele.

Testicular varicoceles are commonly associated with infertility and their correction can help improve the sperm count. The clinician should recall that over 80%

of varicocele cases are not associated with infertility, but up to 40% of men with primary infertility and up to 81% of men with secondary infertility have diagnosed varicoceles.⁴⁹

Varicoceles may be diagnosed via characteristic clinical findings such as scrotal fullness with Valsalva or a “bag of worms” mass that shrinks in the recumbent position and do not require confirmation with grey-scale US, although there is some contention as to whether the diagnosis should be confirmed by doppler. Nevertheless, if the clinical exam findings are equivocal or if an obese body habitus prevents proper examination, it is agreed that doppler imaging can support the diagnosis by demonstrating reversal of venous blood flow with Valsalva or spermatic vein diameter measurement of ≥ 3 mm.⁵⁰ Current practice discourages routine use of US for identification of nonpalpable varicoceles as their repair does not demonstrate clinical benefit.

Venography had the highest sensitivity for varicocele diagnosis and is therefore often used as a gold standard for researchers. However, it is not typically used in general clinical practice as it is both invasive and time consuming (Fig. 27.22).

Cryptorchidism

Cryptorchidism is a congenital disorder involving an undescended testicle and is the most common malformation in newborn males. This irregular positioning of the testes can cause increased risk of infertility as well as testicular cancer, with decreased risk of these disorders in cases of early orchiopexy. On US, cryptorchid testes appear as hypotrophic, inhomogenous, and hypoechoic figures. Although US is the main form of imaging used in cryptorchidism, meta-analyses have reported sonography as an unreliable resource for localization of nonpalpable testes and rule out of intraabdominal testes, with a weak sensitivity and specificity especially in comparison to diagnostic and therapeutic laparoscopy (which has nearly 100% sensitivity and specificity). Imaging is therefore not routinely used to evaluate

Fig. 27.22 Varicocele on doppler US, demonstrating significant refluxing vascular flow with Valsalva⁵¹



differential diagnoses or for preoperative planning prior to orchiopexy, except in cases with obese patients in whom testes palpation is difficult or when searching for Mullerian structures in cases of suspected DSD.

Testicular Hypotrophy

Testicular volume is positively correlated to total sperm count, sperm motility, normal sperm morphology, and testosterone levels. Testicular hypotrophy is defined as a testicular volume less than 12 ml. US has greater precision in measurement of testicular volume than does Prader's orchidometer.

Endnotes

1. Brant W. Diagnostic imaging methods. In: Klein J, Brant W, Helms C, Vinson E, editors. *Fundamentals of diagnostic radiology*, 5th ed. Lippincott Williams & Wilkins; 2012, p. 9–16.
2. Sakamoto H, Saito K, Oohta M, Inoue K, Ogawa Y, Yoshida H. Testicular volume measurement: comparison of ultrasonography, orchidometry, and water displacement. *Urology*. 2007 Jan;69(1):152–7.
3. Dogra VS, Gottlieb RH, Oka M, Rubens DJ. Sonography of the scrotum. *Radiology*. 2003 Apr;227(1):18–36.
4. Cassidy FH, Ishioka KM, McMahon CJ, Chu P, Sakamoto K, Lee KS, et al. MR imaging of scrotal tumors and pseudotumors. *Radiographics*. 2010 May;30(3):665–83.
5. Sweet DE, Feldman MK, Remer EM. Imaging of the acute scrotum: keys to a rapid diagnosis of acute scrotal disorders. *Abdom Radiol (NY)*. 2020 Jul;45(7):2063–81.
6. Di Serafino M, Acampora C, Iacobellis F, Schillirò ML, Borzelli A, Barbuto L, et al. Ultrasound of scrotal and penile emergency: how, why and when. *J Ultrasound*. 2020 Jul 11.
7. Ringdahl E, Teague L. Testicular torsion. *Am Fam Physician*. 2006 Nov 15;74(10):1739–43.
8. Dogra VS, Gottlieb RH, Oka M, Rubens DJ. Sonography of the scrotum. *Radiology*. 2003 Apr;227(1):18–36.
9. Dogra VS, Gottlieb RH, Oka M, Rubens DJ. Sonography of the scrotum. *Radiology*. 2003 Apr;227(1):18–36.
10. Aydogdu O, Burgu B, Gocun PU, Ozden E, Yaman O, Soygur T, et al. Near infrared spectroscopy to diagnose experimental testicular torsion: comparison with Doppler ultrasound and immunohistochemical correlation of tissue oxygenation and viability. *J Urol*. 2012 Feb;187(2):744–50.
11. Di Serafino M, Acampora C, Iacobellis F, Schillirò ML, Borzelli A, Barbuto L, et al. Ultrasound of scrotal and penile emergency: how, why and when. *J Ultrasound*. 2020 Jul 11.
12. Sweet DE, Feldman MK, Remer EM. Imaging of the acute scrotum: keys to a rapid diagnosis of acute scrotal disorders. *Abdom Radiol (NY)*. 2020 Jul;45(7):2063–81.

13. Di Serafino M, Acampora C, Iacobellis F, Schillirò ML, Borzelli A, Barbuto L, et al. Ultrasound of scrotal and penile emergency: how, why and when. *J Ultrasound*. 2020 Jul 11.
14. Sweet DE, Feldman MK, Remer EM. Imaging of the acute scrotum: keys to a rapid diagnosis of acute scrotal disorders. *Abdom Radiol (NY)*. 2020 Jul;45(7):2063–81.
15. Hedayati V, Sellars ME, Sharma DM, Sidhu PS. Contrast-enhanced ultrasound in testicular trauma: role in directing exploration, debridement and organ salvage. *Br J Radiol*. 2012 Mar;85(1011):e65–68.
16. Di Serafino M, Acampora C, Iacobellis F, Schillirò ML, Borzelli A, Barbuto L, et al. Ultrasound of scrotal and penile emergency: how, why and when. *J Ultrasound*. 2020 Jul 11.
17. Di Serafino M, Acampora C, Iacobellis F, Schillirò ML, Borzelli A, Barbuto L, et al. Ultrasound of scrotal and penile emergency: how, why and when. *J Ultrasound*. 2020 Jul 11.
18. Sweet DE, Feldman MK, Remer EM. Imaging of the acute scrotum: keys to a rapid diagnosis of acute scrotal disorders. *Abdom Radiol (NY)*. 2020 Jul;45(7):2063–81.
19. Dogra VS, Gottlieb RH, Oka M, Rubens DJ. Sonography of the scrotum. *Radiology*. 2003 Apr;227(1):18–36.
20. Di Serafino M, Acampora C, Iacobellis F, Schillirò ML, Borzelli A, Barbuto L, et al. Ultrasound of scrotal and penile emergency: how, why and when. *J Ultrasound*. 2020 Jul 11.
21. Dogra VS, Gottlieb RH, Oka M, Rubens DJ. Sonography of the scrotum. *Radiology*. 2003 Apr;227(1):18–36.
22. Sweet DE, Feldman MK, Remer EM. Imaging of the acute scrotum: keys to a rapid diagnosis of acute scrotal disorders. *Abdom Radiol (NY)*. 2020 Jul;45(7):2063–81.
23. Sweet DE, Feldman MK, Remer EM. Imaging of the acute scrotum: keys to a rapid diagnosis of acute scrotal disorders. *Abdom Radiol (NY)*. 2020 Jul;45(7):2063–81.
24. Sharbidre KG, Lockhart ME. Imaging of scrotal masses. *Abdom Radiol (NY)*. 2020 Jul;45(7):2087–108.
25. Parker RA, Menias CO, Quazi R, Hara AK, Verma S, Shaaban A, et al. Mr imaging of the penis and scrotum. *Radiographics*. 2015 Aug;35(4):1033–50.
26. Sharbidre KG, Lockhart ME. Imaging of scrotal masses. *Abdom Radiol (NY)*. 2020 Jul;45(7):2087–108.
27. Ragheb D, Higgins JL. Ultrasonography of the scrotum: technique, anatomy, and pathologic entities. *J Ultrasound Med*. 2002 Feb;21(2):171–85.
28. Ragheb D, Higgins JL. Ultrasonography of the scrotum: technique, anatomy, and pathologic entities. *J Ultrasound Med*. 2002 Feb;21(2):171–85.
29. Park JS, Kim J, Elghiaty A, Ham WS. Recent global trends in testicular cancer incidence and mortality. *Medicine (Baltimore)*. 2018 Sep;97(37):e12390.

30. Sangüesa C, Veiga D, Llavador M, Serrano A. Testicular tumours in children: an approach to diagnosis and management with pathologic correlation. *Insights Imaging*. 2020 May 27;11(1):74.
31. Dogra VS, Gottlieb RH, Oka M, Rubens DJ. Sonography of the scrotum. *Radiology*. 2003 Apr;227(1):18–36.
32. Sharbidre KG, Lockhart ME. Imaging of scrotal masses. *Abdom Radiol (NY)*. 2020 Jul;45(7):2087–108.
33. Kreydin EI, Barrisford GW, Feldman AS, Preston MA. Testicular cancer: what the radiologist needs to know. *AJR Am J Roentgenol*. 2013 Jun;200(6):1215–25.
34. Sharbidre KG, Lockhart ME. Imaging of scrotal masses. *Abdom Radiol (NY)*. 2020 Jul;45(7):2087–108.
35. Sharbidre KG, Lockhart ME. Imaging of scrotal masses. *Abdom Radiol (NY)*. 2020 Jul;45(7):2087–108.
36. Sharbidre KG, Lockhart ME. Imaging of scrotal masses. *Abdom Radiol (NY)*. 2020 Jul;45(7):2087–108.
37. Sharbidre KG, Lockhart ME. Imaging of scrotal masses. *Abdom Radiol (NY)*. 2020 Jul;45(7):2087–108.
38. Sharbidre KG, Lockhart ME. Imaging of scrotal masses. *Abdom Radiol (NY)*. 2020 Jul;45(7):2087–108.
39. Sharbidre KG, Lockhart ME. Imaging of scrotal masses. *Abdom Radiol (NY)*. 2020 Jul;45(7):2087–108.
40. Sharbidre KG, Lockhart ME. Imaging of scrotal masses. *Abdom Radiol (NY)*. 2020 Jul;45(7):2087–108.
41. Sharbidre KG, Lockhart ME. Imaging of scrotal masses. *Abdom Radiol (NY)*. 2020 Jul;45(7):2087–108.
42. Cassidy FH, Ishioka KM, McMahon CJ, Chu P, Sakamoto K, Lee KS, et al. MR imaging of scrotal tumors and pseudotumors. *Radiographics*. 2010 May;30(3):665–83.
43. Dogra VS, Gottlieb RH, Oka M, Rubens DJ. Sonography of the scrotum. *Radiology*. 2003 Apr;227(1):18–36.
44. Ragheb D, Higgins JL. Ultrasonography of the scrotum: technique, anatomy, and pathologic entities. *J Ultrasound Med*. 2002 Feb;21(2):171–85.
45. Ragheb D, Higgins JL. Ultrasonography of the scrotum: technique, anatomy, and pathologic entities. *J Ultrasound Med*. 2002 Feb;21(2):171–85.
46. Balawender K, Orkisz S, Wisz P. Testicular microlithiasis: what urologists should know. A review of the current literature. *Cent European J Urol*. 2018;71(3):310–4.
47. Ragheb D, Higgins JL. Ultrasonography of the scrotum: technique, anatomy, and pathologic entities. *J Ultrasound Med*. 2002 Feb;21(2):171–85.
48. Bieniek JM, Juvet T, Margolis M, Grober ED, Lo KC, Jarvi KA. Prevalence and management of incidental small testicular masses discovered on ultrasonographic evaluation of male infertility. *J Urol*. 2018 Feb;199(2):481–6.

49. Schlegel PN, Sigman M, Collura B, De Jonge CJ, Eisenberg ML, Lamb DJ, et al. Diagnosis and treatment of infertility in men: AUA/ASRM guideline part I. *J Urol*. 2021 Jan;205(1):36–43.
50. Sabanegh A, Agarwal A. Anatomy of the Lower Urinary Tract and Male Genitalia. In: Wein B, Kavoussi L, Novick A, Partin A, Peters C, editors. *Campbell-Walsh urology*, 10th ed. Elsevier Saunders; 2012, p. 628–31.
51. Ragheb D, Higgins JL. Ultrasonography of the scrotum: technique, anatomy, and pathologic entities. *J Ultrasound Med*. 2002 Feb;21(2):171–85.
52. Tasian GE, Copp HL, Baskin LS. Diagnostic imaging in cryptorchidism: utility, indications, and effectiveness. *J Pediatr Surg*. 2011 Dec;46(12):2406–13.

Suggested Further Reading

1. Fulgham P, Bishoff JT. Urinary tract imaging: basic principles. In: Wein B, Kavoussi L, Novick A, Partin A, Peters C, editors. *Campbell-Walsh urology*, 10th ed. Elsevier Saunders; 2012, p. 122–124.
2. Garcia RA, Sajjad H. Anatomy, abdomen and pelvis, scrotum. In: *StatPearls*. StatPearls Publishing; 2020.
3. Wibmer AG, Vargas HA. Imaging of testicular and scrotal masses: the essentials. In: Hodler J, Kubik-Huch RA, von Schulthess GK, editors. *Diseases of the Abdomen and Pelvis 2018–2021*. Springer International Publishing; 2018. p. 257–64.
4. Stephenson A, Eggener SE, Bass EB, Chelnick DM, Daneshmand S, Feldman D, et al. Diagnosis and treatment XE “treatment” of early stage testicular cancer: AUA guideline. *J Urol*. 2019;202(2):272–81.
5. Aoun F, Slaoui A, Naoum E, Hassan T, Albisinni S, Azzo JM, et al. Testicular XE “testicular” microlithiasis: systematic review and clinical guidelines. *Prog Urol*. 2019;29(10):465–73.
6. Jungwirth A, Giwercman A, Tournaye H, Diemer T, Kopa Z, Dohle G, et al. European association of urology guidelines on male infertility XE “infertility”: the 2012 update. *Eur Urol*. 2012;62(2):324–32.